Carbohydrate Polymers 96 (2013) 240–245

Contents lists available at SciVerse ScienceDirect

Carbohydrate Polymers

journal homepage: www.elsevier.com/locate/carbpol

Electrospun carboxymethyl cellulose acetate butyrate (CMCAB) nanofiber for high rate lithium-ion battery

Lei Qiu[a,b], Ziqiang Shao[a,b,*], Mingshan Yang[c], Wenjun Wang[a,b], Feijun Wang[a,b], Long Xie[a,b], Shaoyi Lv[a,b], Yunhua Zhang[a,b]

[a] College of Material Science and Engineering, Beijing Institute of Technology, Beijing 100081, PR China
[b] Beijing Engineering Technology Research Center For Cellulose and Its Derivative Materials, Beijing 100081, PR China
[c] Department of Material Science and Engineering, Beijing Key Lab of Special Elastomer Composites Materials, Beijing Institute of Petrochemical Technology, Beijing 102617, PR China

ARTICLE INFO

Article history:
Received 7 December 2012
Received in revised form 5 March 2013
Accepted 20 March 2013
Available online 28 March 2013

Keywords:
Electrospinning
Cellulose derivatives
Lithium-ion battery
Anode materials LFP

ABSTRACT

Cellulose derivative CMCAB was synthesized, and nanometer fiber composite material was obtained from lithium iron phosphate ($LiFePO_4$, LFP)/CMCAB by electrospinning. Under the protection of inert gas, modified LFP/carbon nanofibers (CNF) nanometer material was obtained by carbonization in 600 °C. IR, TG-DSC, SEM and EDS were performed to characterize their morphologies and structures. LFP/CNF composite materials were assembled into lithium-ion battery and tested their performance. Specific capacity was increased from 147.6 mAh g^{-1} before modification to 160.8 mAh g^{-1} after modification for the first discharge at the rate of 2 C. After 200 charge–discharge cycles, when discharge rate was increased from 2 C to 5 C to 10 C, modified battery capacity was reduced from 152.4 mAh g^{-1} to 127.9 mAh g^{-1} to 106 mAh g^{-1}. When the ratio was reduced from 10 C to 5 C to 2 C, battery capacity can be quickly approximate to the original level. Cellulose materials that were applied to lithium battery can improve battery performance by electrospinning.

1. Introduction

In today's society, lithium-ion battery of circulating charging was recognized as one of the most potential clean batteries for development due to its characteristics of high energy and power. The LFP had advantages of good safety property, long cycle life, wide raw material source, no environmental pollution and so on. So that it has been a hot topic of research and development of anode materials of lithium-ion battery (Kim et al., 2008). Since the electrical conductivity of LFP was extremely low, and diffusion coefficient of Li^+ was small (Raghaven et al., 2008; Wang, Yuan, Wu, Sun, & Huang, 2011b; Yao, Senoh, Sakai, & Kiyobayashi, 2012), which led to the result in poor property of rate of charge and discharge. With the increase of the current density of charge and discharge, there was the phenomenon of capacity of rapid decay. How to improve the electrical conductivity of the material and rate of Li^+ diffusion were two major problems that LFP was faced with. The methods of surface coating, dispersing electronic conductor (Choi et al., 2011; Yang et al., 2012), ion doping (Hellwig, Sorgel, & Bessler, 2011; Sun, Luo, & Fu, 2011; Wu, Zhao, Wang, & Chen, 2011) had a better effect on increasing the conductivity. It not only improved conductivity between the particles, enhanced internal conductivity of LFP particles, and provided an electronic channel for LFP, but also reduced the polarization of the battery. The particle size of LFP in electrode material was the key to improve diffusion capacity of Li^+ in LFP (Yu, Teng, Xie, Cao, & Zhao, 2011).

Cellulose was considered as a biodegradable natural polymer (Zhang & Hsieh, 2008), most of the cellulose derivatives were obtained by etherification or esterification reactions (Figueiredo, Ismael, Anjo, & Duarte, 2010), these materials had unique advantages (Hu & Catchmark, 2011; Oprea et al., 2012; Zadegan, Hosainalipour, Rezaie, Ghassai, & Shokrgozar, 2011). CMCAB was a linear derivative by acidification of cellulose (Amim & Petri, 2012; Blachechen, Souza, & Petri, 2012; Xie, Shao, Wang, & Wang, 2012). It had a structure of multi-carbon functional groups, which could provide abundant carbon resources and obtain a dense conductive carbon structure by modification, and the property laid the foundation for CMCAB in the application of electrochemistry.

Nano LFP was used as an anode material of lithium-ion battery by the method of electrospinning (Lu, Zhou, Liu, & Pan, 2011; Theron, Zussman, & Yarin, 2004), which made anode material have the characteristics of large specific surface area and nano-size effect in order to change material properties (Mai et al., 2010; Wang, Sherman, Verbrugge, & Liu, 2011a; Zhang & Chen, 2011). By

* Corresponding author at: College of Material Science and Engineering, Beijing Institute of Technology, Beijing 100081, PR China. Tel.: +86 10 68940942; fax: +86 10 68941797.
E-mail addresses: qiulei1010@126.com (L. Qiu), Shaoziqiang@263.net (Z. Shao).

0144-8617/$ – see front matter © 2013 Published by Elsevier Ltd.
http://dx.doi.org/10.1016/j.carbpol.2013.03.062

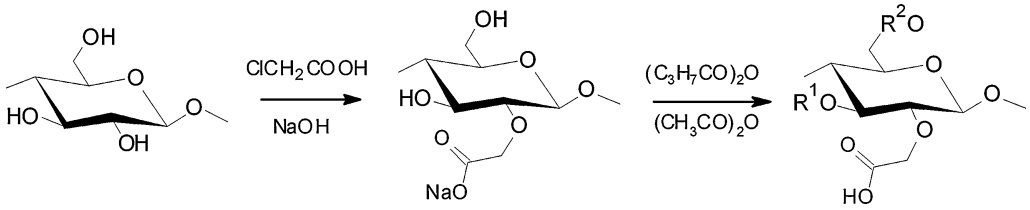

Fig. 1. Synthetic route of CMCAB. Cellulose powder was alkalified and etherified reaction synthesis different content of acyl of CMCAB. CMCAB was a multi-group modified natural polysaccharide derivative.

changing the particle size of LFP, reducing the solid-phase diffusion path of Li^+ and increasing the prolapsed and embedding of Li^+ in order to improve the specific capacity of charge and discharge of LFP. The related research on this method to synthesize cathode material of lithium ion was very few.

In this article, the CMCAB of different structure was synthesized by using special step-by-step reaction control technology. The reaction time was short, and the process was easy to control. Nanometer fiber of CMCAB was obtained by electrospinning, and then we discussed its morphologies and structures. It newly increased the range of polymers that they could be electrically spun. In order to get the more excellent performance of lithium-ion battery cathode material, the common advantages of the two materials were combined, and LFP particles were uniformly dispersed in the new natural polymer cellulose organic acid esters CMCAB substrate by electrospinning. LFP/CNF nanocomposite whose diameter was about 60 nm was obtained by carbonization modification. The study showed that modified LFP particle after carbonization was uniformly dispersed. The performance of the assembled battery was improved in properties of specific capacity, cycle stability, polarization degree and magnification.

2. Experimental

2.1. Materials

Carboxymethyl cellulose acetate butyrate (CMCAB, Mn = 20,000 g/mol) powder was synthesized in our laboratory. CMCAB samples present DSBu = 1.64, DSAc = 0.44, DSCM = 0.33, OH = 0.59. Methylene chloride (MC), monochloroacetic acid, glacial acetic acid, butyric acid, acetone, 98% sulfuric acid, ethanol (EtOH) was supplied by Beijing chemical fine chemical Co. Ltd. (Beijing, China). LFP was kindly supplied by Shanxi power source Co. Ltd. (Taiyuan, Shanxi, China.).

2.2. Synthesis of CMCAB

NaOH solution, 600 mL isopropyl alcohol–ethanol–water solvent of certain proportion and 30 g cellulose powder were added to a flask. The solution was constantly stirred up and alkalified 1.5 h at 20 °C, while controlling the feed speed, 10 g chloroacetic acid was slowly added. The solution was etherified 2 h at 40–70 °C, and the required carboxyl methyl cellulose (CMC) was obtained by neutralizing, washing and drying. 30 g CMC was added to a flask and acidized 1 h with a dilute solution of 10% sulfuric acid, and then a certain amount of esterifying agent and catalyst was added into the solvent. It was esterified 2 h in stages at 35–70 °C, the product was obtained by hydrolysis, precipitation, filtration, washing with water and drying. The different content of acyl of CMCAB was obtained by adjusting the ratio of acetic anhydride and butyric anhydride for esterification reaction. Synthetic route was shown in Fig. 1.

2.3. Electrospinning

CMCAB was dissolved in a mixed solvent of ethanol and dichloromethane, which was divided into A and B in duplicate. LFP was added into solvent B, intermittent ultrasound concussion 10 min later, when CMCAB was completely dissolved, nano CMCAB fiber and LFP/CMCAB fiber were obtained by electrospinning device. Processing conditions were adjusted to a flow rate of 4 mL/h, an applied voltage of 25 kV, a capillary tip-to-target distance of 10 cm and a temperature of 25 °C. The CMCAB/LFP composite fiber at a high temperature under the protection of inert gas (600 °C) was carbonized 2 h to obtain a modified LFP/CNF nanocomposites, and then button 2032 lithium-ion battery was assembled for performance testing.

2.4. Characterization

Fourier transforms infrared spectroscopy (FT-IR) spectra of CMC and CMCAB powders were recorded on a Nicolet 6700 infrared spectrometer (USA) with resolution of 2 cm^{-1} at room temperature. The dried powder was measured with a Ker-pellet method in the range of 4000–500 cm^{-1}. The morphology and structure of electrospun CMCAB fibers were observed with a scanning electron microscope (SEM, JSM-6700F) after gold coating. Electrochemical workstation: CHI660D, Shanghai Chen Hua Instrument Co. Ltd.; Battery test system: BTS-5V10mA, Shenzhen Neware Electronics Co. Ltd.

3. Results and discussion

3.1. The analysis of IR spectrogram

From the view of spectrogram Fig. 2, it showed that a sharp absorption peak at the place of 1580 cm^{-1} and 1400 cm^{-1} was the anti-symmetric and symmetric stretching vibration peak of —COO, it was characteristic absorption peaks after carboxylic acid to salt, and it also confirmed the formation of the intermediate

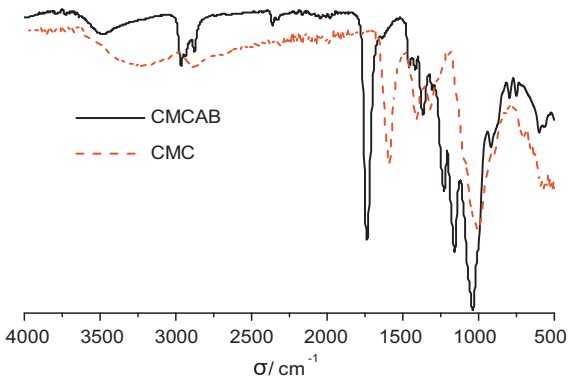

Fig. 2. IR Spectra for CMCAB and CMC. CMC and new cellulose derivatives CMCAB were successfully synthesized. By the analysis of IR spectrogram, it also confirmed the formation of the intermediate products of CMC, and last products CMCAB.

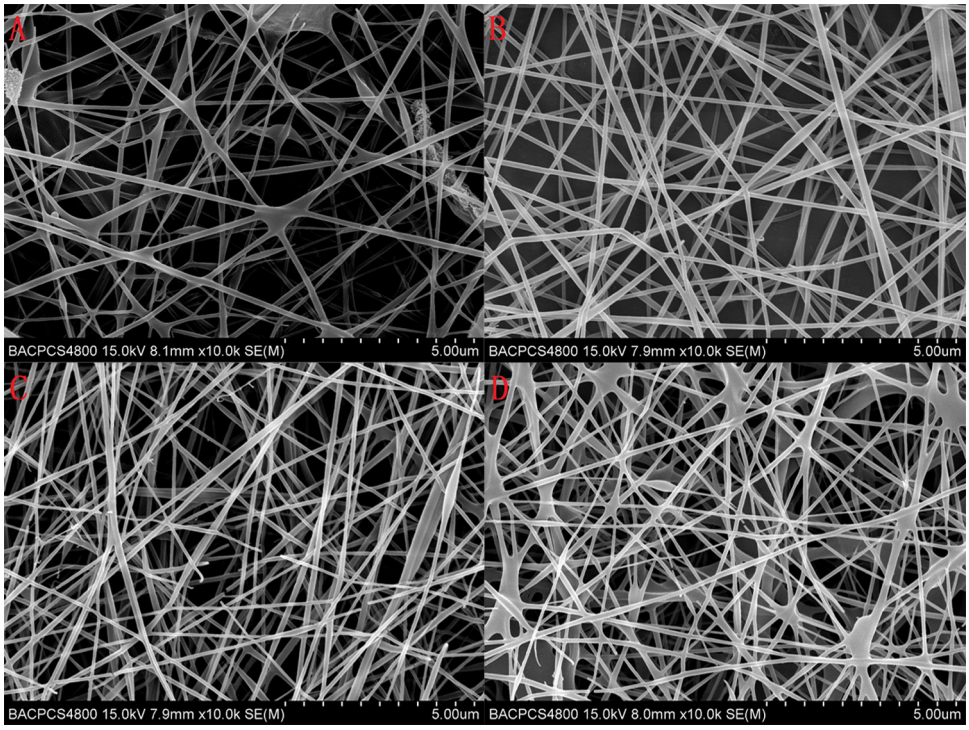

Fig. 3. SEM photos at two different the mass ratio of dichloromenthane: ethanol solvents of electrospun CMCAB nanofibers. The new cellulose derivatives CMCAB was successfully electrospun for the first time by using mixed solvents. The mass ratio of solvent dichloromethane: ethanol was 9:1, 4:1, 7:3 and 6:4, when other spinning conditions remained unchanged. Choose the best solvent ratio.

products of CMC. However, the characteristic peaks of CMC disappeared after acidification and esterification. And there was a strong sharp absorption peak of carbonyl C=O to illustrate the formation of CMCAB.

Meanwhile, compared with the single peak in the 2800 cm^{-1} of CMC, there were stretching vibrations of methylene $-CH_2-$ and methyl-CH_3 in the 2870 cm^{-1} and 2960 cm^{-1} of CMCAB, so that the existence of ester, acetyl and betrayal can be proven. In

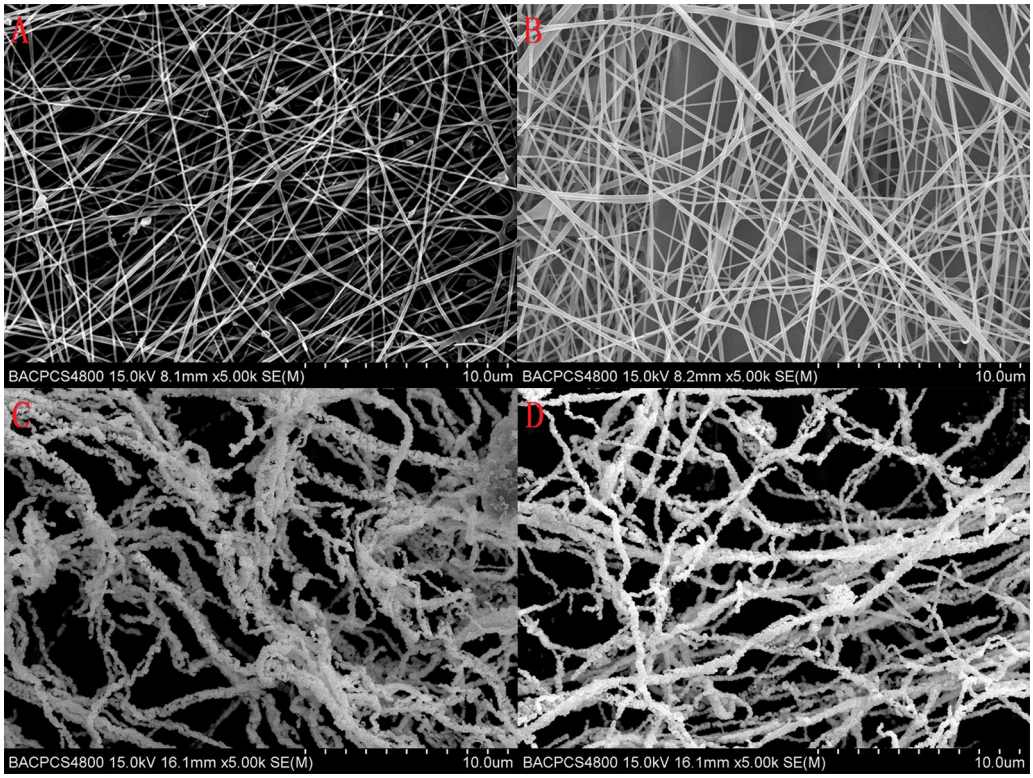

Fig. 4. SEM photos of LFP/CMCAB composite fibers before and after carbonization. Preparation LFP/CMCAB nanometer composite fiber, and high-temperature carbonization modified LFP/CNF coated nanocomposites.

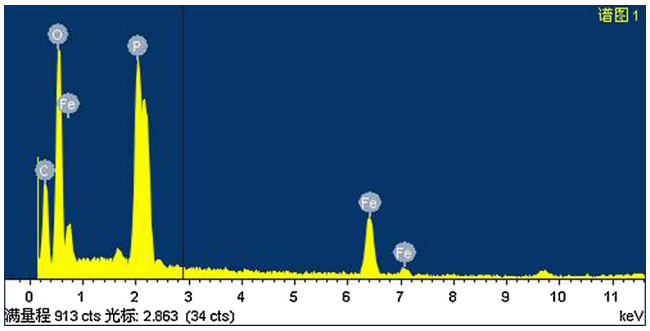

Fig. 5. EDS Spectrum of LFP/CMCAB composite materials (after carbonization). Fiber materials contained the elements of P, C, O and Fe after carbonization, and it showed that LFP in composite fiber materials was equably dispersed in the entire spun fibers and formed nanocomposites of LFP, which was coated with carbon.

addition, there were asymmetric stretching vibration and symmetric stretching vibration of C—O—C in the 1220 cm^{-1}, 1150 cm^{-1} and 1030 cm^{-1} to further prove the existence of ester. Moreover, broad peak of —OH in 3400 cm^{-1} of CMC was significantly reduced after esterification.

3.2. Electrospinning of CMCAB nano fibers

The electrospinning solvent had an important effect on formation of fiber, diameter and surface morphology. Fig. 3 shows that nano CMCAB fiber was obtained by using mixed solvents, the mass ratio of solvent dichloromethane and ethanol was 4:1 and other spinning conditions remained unchanged. The surface of the fiber was relatively smooth. The thickness was relatively uniform, and there was no formation of the larger link or particularly messy breakpoints. All of these proved that the spinning process was more stable.

3.3. SEM photos of composite fibers

Fig. 4 shows that there were four SEM photographs before and after carbonation of LFP/CMCAB nano-composite material. It can be seen that LFP particles were equably dispersed in the fiber matrix after carbonation, and then formed the compound coating material of LFP/CNF. Because of the small particle size, it can solve the problem of low tap density of LFP anode materials after compaction processing. While the uniform distribution of LFP/CNF composite material was due to the fact that the particle in the spinning solution was continuing to keep down by fiber template. A good solution to the problem of poor conductivity and the decline of battery performance in the lithium-ion battery was due to the fact of uneven distribution of graphite.

3.4. Analysis of energy diffraction spectrum (EDS)

Fig. 5 shows that there was an EDS spectrogram of any point after carbonization of LFP/CMCAB. It can be seen that fiber materials contained the elements of P, C, O and Fe after carbonization. LFP in composite fiber materials was equably dispersed in the entire spun fibers and formed nanocomposites of LFP, which was coated with carbon.

3.5. Analysis of precursor TG-DSC in different temperature

Fig. 6 shows that water began to be prolapsed and cellulose derivatives began to be dissolved in the weightlessness interval of range from room temperature to 220 °C. When the temperature was increased from 220 °C to 600 °C, organic polymer CMCAB began to be dissolved by heat. In this process, it was known by

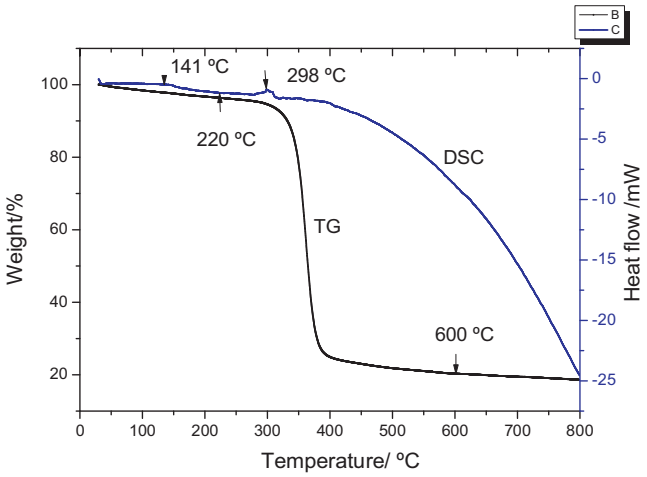

Fig. 6. The TG-DSC curves of LFP nano-fiber precursor in nitrogen. Find the carbonization temperature and thermal analysis of composite materials.

the DSC diagram that there was an exothermic peak in the place of 298 °C, which may correspond to the decomposition of organic polymer CMCAB, and its corresponding weightlessness was about 16%, which was consistent with the amount of CMCAB in the starting material. After 600 °C, it began to enter a state of constant weight and only LFP was generated. We can see from the above analysis that the synthesis temperature should be at least above 600 °C in order to obtain the well crystallized LFP.

3.6. Property of charge and discharge

It can be easily seen from Fig. 7 that the charge–discharge capacity of LFP/CNF (modified LFP) was higher than that of pure LFP, which was used as anode materials. We can draw the conclusion that the method of electrospinning can effectively improve the active utilization of LFP with cellulose derivatives in electrode. In addition, it was due to the fact that the distance between charging platform of modified LFP electrode material was smaller than that of pure LFP to prove that the degree of polarization became lower, the efficiency of charging was improved.

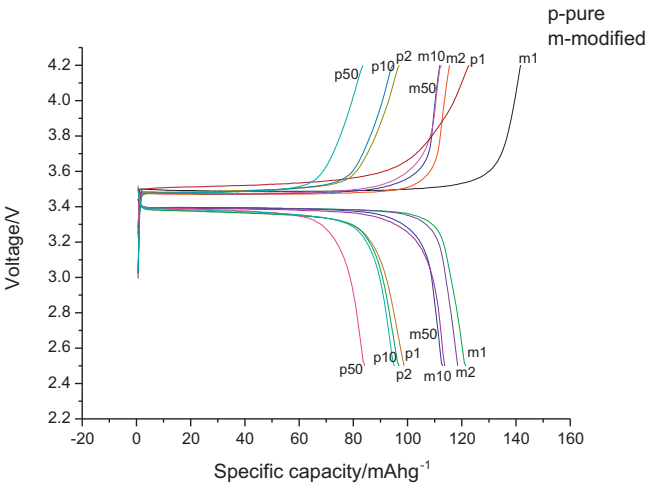

Fig. 7. Charge–discharge curve of pure and modified LFP Lithium electrode in different rate. The charge–discharge capacity of LFP/CMCAB (modified LFP) was higher than that of pure LFP, which was used as anode materials.

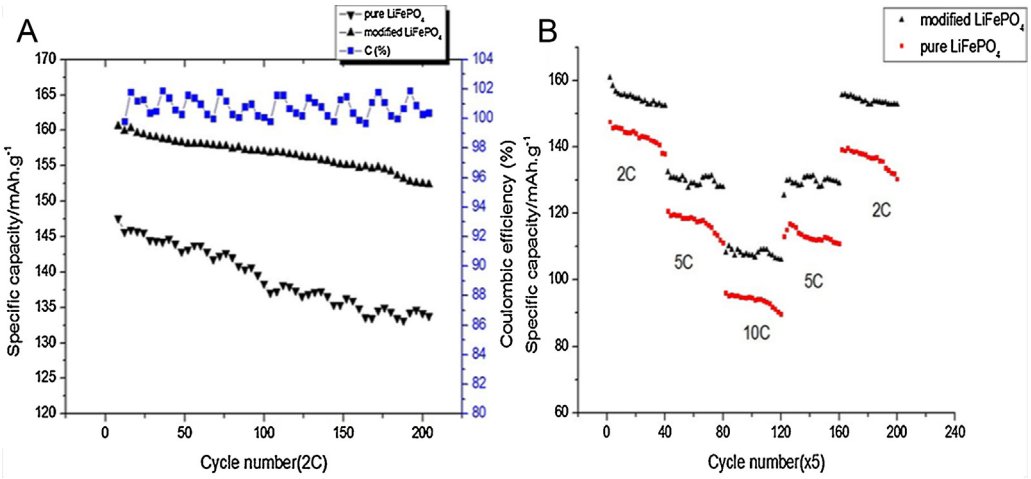

Fig. 8. The discharge/charge capacity cycle curves of cells with two electrode materials. (A) The first discharge/charge curves of the cells at 2 C rate. (B) The discharge/charge cycle curves of cells at the different rate. Such excellent rate performance strongly confirmed that it cannot only enhance the cycle stability of material, but also improve the rate property of electrode materials by LFP/CNF modification with cellulose derivative material.

3.7. Property of the cycle

After 200 charge–discharge cycles, discharge capacities were 130.8 mAh g^{-1} and 152.4 mAh g^{-1}. Capacity attenuation was reduced from 11.38% to 5.11%. Fig. 8B shows after the 200 charge–discharge cycles, as the discharge–charge rate increased from 2 C to 10 C, the discharge capacities of LFP/CNF demonstrated remarkable rate capability. Delivering a discharge capacity of 152.4 mAh g^{-1}, 127.9 mAh g^{-1} and 106 mAh g^{-1} at 2, 5 and 10 C, respectively. As the discharge–charge rate reduced from 10 C to 2 C, capacity can be quickly approximate to its original level. Such excellent rate performance strongly confirmed that it cannot only enhance the cycle stability of material, but also improve the rate property of electrode materials by LFP/CNF modification with cellulose derivative material. There may be two reasons, on one hand, as the surface of LFP was evenly coated by CMCAB, and LFP/CNF was formed after carbonization to enhance the conductivity of materials. On the other hand, Ionic conductivity of LFP was related to the size of particles. The smaller the particle was, the shorter the transmission channel of lithium ion in LFP became. The faster lithium ion can come in and out, the better the property of battery will be.

4. Conclusions

1D net architectures of LFP/CMCAB fibers have been successfully prepared by electrospinning technique. LFP was nano characterized and carbonized. LFP particles were distributed within the fibers uniformly, modified LFP/CNF nanometer composite material was obtained by carbonization in 600 °C. By reducing the conduction path of lithium-ion and improving the efficiency of penetration can improve the capacity, cycle properties, rate properties of LFP, which was used as a battery anode. The discharge capacity of electrospun CNF/LFP electrode material for the first cycle at the rate of 2 C was 160.6 mAh g^{-1}. After the 200 charge–discharge cycle, as the discharge–charge rate increased from 2 C to 10 C, and the rate was reduced from 10 C to 2 C, capacity can be quickly approximate to its original level. Such excellent rate performance strongly confirmed that the electrospun LFP nonwoven films composed of oriented arrays of fibers are highly promising as binder and conductive additive-free film electrodes for lithium-ion battery anode material in CMCAB. The increase of the material surface structure of the current collector is critical to achieve high electrode performance.

Acknowledgement

This work was financially supported by the Natural Science Foundation of Beijing.

References

Amim, J., Jr., & Petri, D. F. S. (2012). Effect of amino-terminated substrates onto surface properties of cellulose esters and their interaction with lectins. *Materials Science and Engineering C: Materials for Biological Applications*, *32*(2), 348–355.

Blachechen, L. S., Souza, M. A., & Petri, D. F. S. (2012). Effect of humidity and solvent vapor phase on cellulose esters films. *Cellulose*, *19*(2), 443–457.

Choi, J. W., Manuel, J., Ha, J. K., Cho, K. K., Kim, K. W., & Ahn, J. H. (2011). Electrochemical properties of nano-sized $LiFePO_4$ materials prepared by hydrothermal method for lithium batteries. *Journal of Ceramic Processing Research*, *12*, S101–S104.

Figueiredo, J. A., Ismael, M. I., Anjo, C. M. S., & Duarte, A. P. (2010). Cellulose and derivatives from wood and fibers as renewable sources of raw-materials. In A. P. Rauter, P. Vogel, & Y. Queneau (Eds.). Carbohydrates in sustainable development I: Renewable resources for chemistry and biotechnology. *Topics in Current Chemistry*, *294*, 117–128. http://dx.doi.org/10.1007/128_2010_88

Hellwig, C., Sorgel, S., & Bessler, W. G. (2011). A multi-scale electrochemical and thermal model of a $LiFePO_4$ battery. In M. C. Smart, A. Manivannan, P. N. Kumta, & S. R. Narayan (Eds.). Battteries and energy technology (general)-219th ecs meeting. *Ecs Transactions*, *35*(32), 215–228. http://dx.doi.org/10.1149/1.3655705

Hu, Y., & Catchmark, J. M. (2011). Integration of cellulases into bacterial cellulose: Toward bioabsorbable cellulose composites. *Journal of Biomedical Materials Research Part B: Applied Biomaterials*, *97B*(1), 114–123.

Kim, J.-K., Cheruvally, G., Li, X., Ahn, J.-H., Kim, K.-W., & Ahn, H.-J. (2008). Preparation and electrochemical characterization of electrospun, microporous membrane-based composite polymer electrolytes for lithium batteries. *Journal of Power Sources*, *178*(2), 815–820.

Lu, F., Zhou, Y. C., Liu, J., & Pan, Y. (2011). Enhancement of F-doping on the electrochemical behavior of carbon-coated LiFePO(4) nanoparticles prepared by hydrothermal route. *Electrochimica Acta*, *56*(24), 8833–8838.

Mai, L., Xu, L., Han, C., Xu, X., Luo, Y., Zhao, S., et al. (2010). Electrospun ultralong hierarchical vanadium oxide nanowires with high performance for lithium ion batteries. *Nano Letters*, *10*(11), 4750–4755.

Oprea, A.-M., Profire, L., Lupusoru, C. E., Ghiciuc, C. M., Ciolacu, D., & Vasile, C. (2012). Synthesis and characterization of some cellulose/chondroitin sulphate hydrogels and their evaluation as carriers for drug delivery. *Carbohydrate Polymers*, *87*(1), 721–729.

Raghaven, P., Choi, J.-W., Ahn, J.-H., Cheruvally, G., Chauhan, G. S., Ahn, H.-J., et al. (2008). Novel electrospun poly(vinylidene fluoride-co-hexafluoropropylene)-in situ SiO_2 composite membrane-based polymer electrolyte for lithium batteries. *Journal of Power Sources*, *184*(2), 437–443.

Sun, Q., Luo, J. Y., & Fu, Z. W. (2011). Facile synthesis and electrochemical properties of carbon-coated LiCoPO(4) submicron particles as positive materials for lithium ion batteries. *Electrochemical and Solid State Letters*, *14*(10), A151–A153.

Theron, S. A., Zussman, E., & Yarin, A. L. (2004). Experimental investigation of the governing parameters in the electrospinning of polymer solutions. *Polymer*, *45*(6), 2017–2030.

Wang, J. S., Sherman, E., Verbrugge, M., & Liu, P. (2011). Composite electrodes of disordered carbon and graphite for improved battery state estimation with minimal performance penalty. *Journal of Power Sources*, *196*(22), 9648–9653.

Wang, Z. H., Yuan, L. X., Wu, M., Sun, D., & Huang, Y. H. (2011). Effects of Na+ and Cl− co-doping on electrochemical performance in $LiFePO_4$/C. *Electrochimica Acta*, *56*(24), 8477–8483.

Wu, C. R., Zhao, C. C., Wang, Z. X., & Chen, L. Q. (2011). Li-rich layer-structured cathode materials for Li-ion batteries. *Progress in Chemistry*, *23*(10), 2038–2044.

Xie, L., Shao, Z., Wang, W., & Wang, F. (2012). Superhydrophobicity of CMCAB fibrous mats produced by electrospinning. *Integrated Ferroelectrics*, *135*, 55–61.

Yang, J., Wang, J., Li, X., Wang, D., Liu, J., Liang, G., et al. (2012). Hierarchically porous $LiFePO_4$/nitrogen-doped carbon nanotubes composite as a cathode for lithium ion batteries. *Journal of Materials Chemistry*, *22*(15), 7537–7543.

Yao, M., Senoh, H., Sakai, T., & Kiyobayashi, T. (2012). Redox active poly(N-vinylcarbazole) for use in rechargeable lithium batteries. *Journal of Power Sources*, *202*, 364–368.

Yu, H. M., Teng, X. B., Xie, J. A., Cao, G. S., & Zhao, X. B. (2011). In situ one-step synthesis of LiFePO(4)/carbon-fiber by a self-catalyzed growth route. *Electrochemical and Solid State Letters*, *14*(2), A19–A21.

Zadegan, S., Hosainalipour, M., Rezaie, H. R., Ghassai, H., & Shokrgozar, M. A. (2011). Synthesis and biocompatibility evaluation of cellulose/hydroxyapatite nanocomposite scaffold in 1-n-allyl-3-methylimidazolium chloride. *Materials Science and Engineering C: Materials for Biological Applications*, *31*(5), 954–961.

Zhang, L. C., & Chen, C. H. (2011). Electrode materials for lithium ion battery. *Progress in Chemistry*, *23*(2–3), 275–283.

Zhang, L., & Hsieh, Y.-L. (2008). Ultra-fine cellulose acetate/poly(ethylene oxide) bicomponent fibers. *Carbohydrate Polymers*, *71*(2), 196–207.